

F-theory duals of singular heterotic K3 models

Christoph Lüdeling^{a,1}, Fabian Ruehle^{b,2}

^a Institut für Gebirgsmechanik GmbH, Friederikenstraße 60, 04279 Leipzig, Germany

^b Deutsches Elektronen-Synchrotron DESY, Notkestrasse 85, 22607 Hamburg, Germany

Abstract

We study F-theory duals of singular heterotic K3 models that correspond to abelian toroidal orbifolds T^4/\mathbb{Z}_N . While our focus is on the standard embedding, we also comment on models with Wilson lines and more general gauge embeddings. In the process of constructing the duals, we work out a Weierstrass description of the heterotic toroidal orbifold models, which exhibit singularities of Kodaira type I_0^* , IV^* , III^* , and II^* . This construction unveils properties like the instanton number per fixed point and a correlation between the orbifold order and the multiplicities in the Dynkin diagram. The results from the Weierstrass description are then used to restrict the complex structure of the F-theory Calabi–Yau threefold such that the gauge group and the matter spectrum of the heterotic theories are reproduced. We also comment on previous approaches that have been employed to construct the duality and point out the differences to our case. Our results show explicitly how the various orbifold models are connected and described in F-theory.

¹E-mail: christoph.luedeling@gmail.com

²E-mail: fabian.ruehle@desy.de

Contents

1	Introduction	1
2	Review of heterotic – F-theory duality	2
2.1	6D heterotic orbifold models	2
2.2	Dual F-theory constructions	4
2.3	Heterotic – F-theory duality in the smooth case	6
2.4	Comparison with other singular K3 limits	9
3	F-theory duals of heterotic orbifold models	11
3.1	Constructing the duals of the T^4/\mathbb{Z}_2 orbifold	12
3.2	Constructing the duals of the T^4/\mathbb{Z}_3 orbifold	15
3.3	Constructing the duals of the T^4/\mathbb{Z}_4 orbifold	17
3.4	Constructing the duals of the T^4/\mathbb{Z}_6 orbifold	19
3.5	Constructing the duals of T^4/\mathbb{Z}_N orbifolds with Wilson lines	21
3.6	General instanton embedding	22
4	Conclusions and outlook	23

1 Introduction

Heterotic $E_8 \times E_8$ orbifold models [1–3] are popular for string phenomenology and for physics beyond the standard model [4–8]. Heterotic toroidal abelian orbifolds are based on tori which are orbifolded by acting with discrete abelian groups \mathbb{Z}_N or $\mathbb{Z}_N \times \mathbb{Z}_M$. This introduces mild singularities at the fixed points, which reduces the amount of parallelizable spinors and can thus lead to models with reduced supersymmetry in lower dimensions. Compatibility with the discrete action fixes the complex structure of the underlying tori (except for the case of \mathbb{Z}_2). These models are based on free conformal field theories which allow for an exact treatment. Orbifolds are at rather special points in the moduli space of string compactifications which exhibit enhanced symmetry. In particular, the primordial $E_8 \times E_8$ gauge group is broken rank-preservingly. Furthermore, there are many discrete symmetries which can help solving problems inherent to most models beyond the Standard Model such as proton decay or the μ -problem [9]. This makes orbifolds phenomenologically attractive, but also rather special points, apparently isolated from each other and from smooth (supergravity) compactifications. In the last years there has been considerable progress connecting different orbifolds with their smooth supergravity counterparts [10–12]; however, the process has to be carried out for each orbifold separately.

F-Theory [13] was introduced roughly ten years later as an approach to constructing string vacua which are connected via a web of dualities to type II and heterotic string theories. While these dualities have been worked out for various dimensions of string compactification spaces, we focus on the case of orbifolds corresponding to singular K3 surfaces on the heterotic side, which correspond to F-theory models on (elliptically fibered) Calabi–Yau (CY) threefolds over a

complex two-dimensional base space which is a Hirzebruch surface \mathbb{F}_m [14,15]. Most commonly, the elliptically fibered CY threefolds are discussed in terms of a Weierstrass model, in which the elliptic fiber is given in terms of an equation of degree 6 in the weighted projective space \mathbb{P}_{231}^2 whose coefficients are sections in the base \mathbb{F}_m . Generically, the elliptic fiber degenerates over codimension one subloci in the base. The resolution of the singularities were classified by Kodaira [16] in terms of the vanishing orders of the coefficients f, g , and the discriminant Δ of the Weierstrass equation. The resolution requires the introduction of \mathbb{P}^1 's whose intersection numbers are those of the negative affine Cartan matrix of the ADE-type Lie algebras. Using F-/M-theory duality, it can be seen that the ADE-type singularities give rise to precisely the same gauge group in F-theory. For this reason, we use the name of the singularity in the Kodaira classification and the name of the resulting gauge algebra somewhat interchangeably. Matter arises in codimension two where the singularity type of the fiber is further enhanced. In the meantime, there has been quite some progress in string phenomenology based on F theory, ultimately motivated by the possibility to obtain exceptional groups and more general matter representations than in type IIB intersecting brane models. Similar to intersecting branes, however, much of the phenomenological work discusses local models, and global completions are much harder to construct.

For the F-theory duals of smooth models, there is a general algorithm for the construction [17–19]. In contrast, F-/M-Theory on singular spaces is less well understood [20–22]. As we shall see, also in our case the tools from the smooth case cannot be applied directly (cf. also [23]). Furthermore, as we shall explain, toroidal orbifolds do not have a direct Weierstrass description. To circumvent this problem we will use a method used in [24] to construct a Weierstrass model and from that the heterotic–F-theory duality.

The rest of the paper is organized as follows: In section 2 we review heterotic orbifold models, F-theory, and the construction of the duality. In the process, we compare to other methods used to construct the duals in the smooth case. In section 3 we construct the F-theory duals of all four T^4/\mathbb{Z}_N orbifolds in the “standard embedding” (which means in the case of orbifolds that the discrete gauge bundle is \mathbb{Z}_N , leading to a commutant of $E_7 \times \text{SU}(2)$ for $N = 1$ or $E_7 \times \text{U}(1)$ for $N = 3, 4, 6$, respectively) and comment on cases with more general gauge embeddings. In section 4 we conclude and present an outlook.

2 Review of heterotic – F-theory duality

2.1 6D heterotic orbifold models

We consider heterotic orbifold compactifications to six dimensions on Calabi–Yau manifolds, which are singular limits of K3. We study orbifolds of the type T^4/\mathbb{Z}_N with $N = 2, 3, 4, 6$. The spectra and gauge groups that can be obtained in these models without using Wilson lines have been classified in [25]. We collect the spectra of the standard embeddings in table 1. We also included the spectrum of a T^4/\mathbb{Z}_2 orbifold where one Wilson line in the first torus has been switched on. This Wilson line has two effects: It breaks the gauge group further down (while preserving the rank) and it projects out some of the matter states which are incompatible with

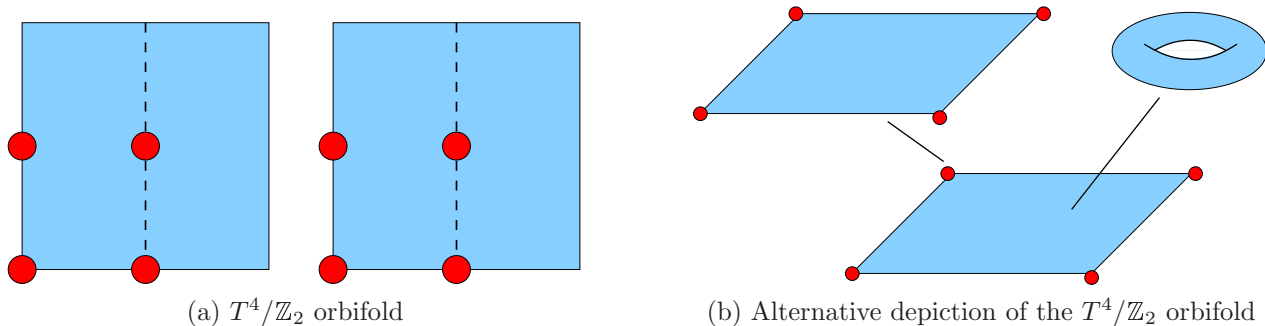


Figure 1: Picture of the T^4/\mathbb{Z}_2 orbifold. The $4 \times 4 = 16$ fixed points are drawn as red dots. The second picture gives an alternative depiction, which will be useful when constructing the F-theory dual later.

the Wilson line. This leads to the fact that the spectrum at the various orbifold fixed points where the Wilson line acts is different from the spectrum where the Wilson line is trivial.

For our discussion, we will start with the most simple model, which is the standard embedding of T^4/\mathbb{Z}_N with gauge group $(E_7 \times SU(2)) \times E_8$ or $(E_7 \times U(1)) \times E_8$. The orbifold acts on the two complex torus coordinates (z_1, z_2) as

$$\theta : (z_1, z_2) \mapsto (e^{2i\pi/N} z_1, e^{-2i\pi/N} z_2). \quad (1)$$

In order to ensure modular invariance, a twist by $v = \frac{1}{N}(1, -1)$ in a T^4/\mathbb{Z}_N orbifold in standard embedding is accompanied by a shift in the $E_8 \times E_8$ gauge degrees of freedom by $V = \frac{1}{N}(1, -1, 0^6)(0^8)$. For the T^4/\mathbb{Z}_2 model this means that the orbifold acts as a reflection, $(z_1, z_2) \mapsto (-z_1, -z_2)$ and the associated shift breaks the gauge group to $(E_7 \times SU(2)) \times E_8$. The orbifold action introduces four fixed points in each torus, leading to 16 \mathbb{Z}_2 (or A_1) orbifold singularities, cf. figure 1. Comparing with table 1, we see that there are eight $(\mathbf{56}, \mathbf{1})$. Note, however, that the $\mathbf{56}$ of E_7 is pseudo-real, so there are 16 half-hypers, i.e. one per fixed point. Likewise, there are 32 hypermultiplet doublets $(\mathbf{1}, \mathbf{2})$ which are pseudo-real as well, leading to 4 half-hypers per fixed point. In contrast, the $(\mathbf{56}, \mathbf{2})$ and the four singlets $(\mathbf{1}, \mathbf{1})$ in the untwisted sector are not pseudo-real and thus are full hypermultiplets. Also note that there is no matter charged under the second (unbroken) E_8 . It should be mentioned that the subtlety concerning pseudo-real representations mainly arise in the T^4/\mathbb{Z}_2 models. The reason is that the commutant of \mathbb{Z}_N with E_8 for $N \neq 2$ is $U(1)$ rather than $SU(2)$. For that reason, the other orbifold standard embeddings come with a $U(1)$ factor, and thus the irreps carrying $U(1)$ charge are complex (but e.g. the 5 singlets of the \mathbb{Z}_4 model are uncharged and correspond to 10 half-hypers at the 6+4 \mathbb{Z}_2 fixed points occurring in the second twisted sector of \mathbb{Z}_4). In fact, in all cases where the number of states is half the number of equivalent fixed points the representations are pseudo-real, such that there is one half-hyper per fixed point.

An advantage of 6D $\mathcal{N} = 1$ models is that the chirality of the spinors is fixed: the chirality of the hypermultiplets and tensor multiplets is the same and opposite to the chirality of the vector multiplets. This leads to very stringent anomaly cancellation conditions. In particular, the gravitational anomaly reads

$$N_H - N_V + 29N_T = 273, \quad (2)$$

Orbifold	Gauge Group	Untwisted matter	Twisted matter
T^4/\mathbb{Z}_2	$E_7 \times SU(2) \times E_8$	$(\mathbf{56}, \mathbf{2}) + 4(\mathbf{1}, \mathbf{1})$	$8(\mathbf{56}, \mathbf{1}; \mathbf{1}) + 32(\mathbf{1}, \mathbf{2})$
	$SO(12) \times SU(2)^2 \times E_8$	$(\mathbf{12}, \mathbf{2}, \mathbf{2}) + 4(\mathbf{1}, \mathbf{1}, \mathbf{1})$	$4(\mathbf{32}, \mathbf{1}, \mathbf{1}) + 4(\mathbf{12}, \mathbf{2}, \mathbf{1}) + 16(\mathbf{1}, \mathbf{1}, \mathbf{2}) + 4(\mathbf{32}, \mathbf{1}, \mathbf{1}) + 4(\mathbf{12}, \mathbf{1}, \mathbf{2}) + 16(\mathbf{1}, \mathbf{2}, \mathbf{1})$
T^4/\mathbb{Z}_3	$E_7 \times U(1) \times E_8$	$(\mathbf{56})_1 + (\mathbf{1})_2 + 2(\mathbf{1})_0$	$9(\mathbf{56})_{\frac{1}{3}} + 45(\mathbf{1})_{\frac{2}{3}} + 18(\mathbf{1})_{\frac{4}{3}}$
T^4/\mathbb{Z}_4	$E_7 \times U(1) \times E_8$	$(\mathbf{56})_1 + 2(\mathbf{1})_0$	$4(\mathbf{56})_{-\frac{1}{2}} + 8(\mathbf{1})_{\frac{3}{2}} + 24(\mathbf{1})_{\frac{1}{2}} + 5(\mathbf{56})_0 + 32(\mathbf{1})_1$
T^4/\mathbb{Z}_6	$E_7 \times U(1) \times E_8$	$(\mathbf{56})_1 + 2(\mathbf{1})_0$	$1(\mathbf{56})_{-\frac{2}{3}} + 8(\mathbf{1})_{\frac{1}{3}} + 2(\mathbf{1})_{-\frac{5}{3}} + 5(\mathbf{56})_{-\frac{1}{3}} + 22(\mathbf{1})_{\frac{2}{3}} + 10(\mathbf{1})_{-\frac{4}{3}} + 3(\mathbf{56})_0 + 22(\mathbf{1})_1$

Table 1: Spectrum of T^4/\mathbb{Z}_N orbifold models. Except for the model in the second line, which has one Wilson line, all models are in the orbifold standard embedding. In all models, the second E_8 is unbroken, so we omit it in the irreps for brevity. For \mathbb{Z}_4 and \mathbb{Z}_6 , the i^{th} line corresponds to the matter contribution of the i^{th} twisted sector.

where N_H, N_V, N_T are the number of hyper-, vector-, and tensor multiplets. Perturbative heterotic string models always have $N_T = 1$, where the scalar of the tensor multiplet is the dilaton. Using (2) and the other conditions ensuring the absence of gauge and mixed anomalies, it can be easily checked that the models in table 1 are anomaly-free. Note that in contrast to 4D, the anomaly (2) also depends on the singlets, i.e. it is sensitive to the entire particle spectrum.

It is well-known that these singularities can be resolved, leading to heterotic string models on smooth Calabi–Yaus with vector bundles. In the case of the standard embedding, the vector bundle is $SU(2)$ which breaks the $E_8 \times E_8$ to the commutant $E_7 \times E_8$. The heterotic Bianchi identity for the Kalb–Ramond three-form field strength reads

$$dH = \text{ch}_2(TX) - \text{ch}_2(V). \quad (3)$$

Since the instanton number (i.e. the second Chern class) of K3 is 24, we need to embed a total of 24 instantons in the gauge bundle to satisfy this identity. In principle, (3) is modified in the presence of Neveu–Schwarz five-branes. Including these five-branes will lead to F-theory duals with more than one tensor multiplet¹, but we will not say too much about this.

2.2 Dual F-theory constructions

F-theory models on Calabi–Yau threefolds X with a heterotic dual show a special fibration structure [14, 15]. They are K3 fibrations over \mathbb{P}^1 , where the K3 is itself elliptically fibered over another \mathbb{P}^1 . The base space B of the elliptically fibered CY threefold, i.e. the \mathbb{P}^1 fibration over \mathbb{P}^1 , corresponds to a Hirzebruch surface \mathbb{F}_m . The situation is depicted in figure 2.

Some of the particle content of the underlying theory is fixed by the geometrical data of the CY threefold and the base space [13, 15]. Using, among other things, that in going from the 6D

¹The scalar in these extra tensor multiplets encodes the position of the five-brane in the M-theory bulk, as explained in section 3.6.

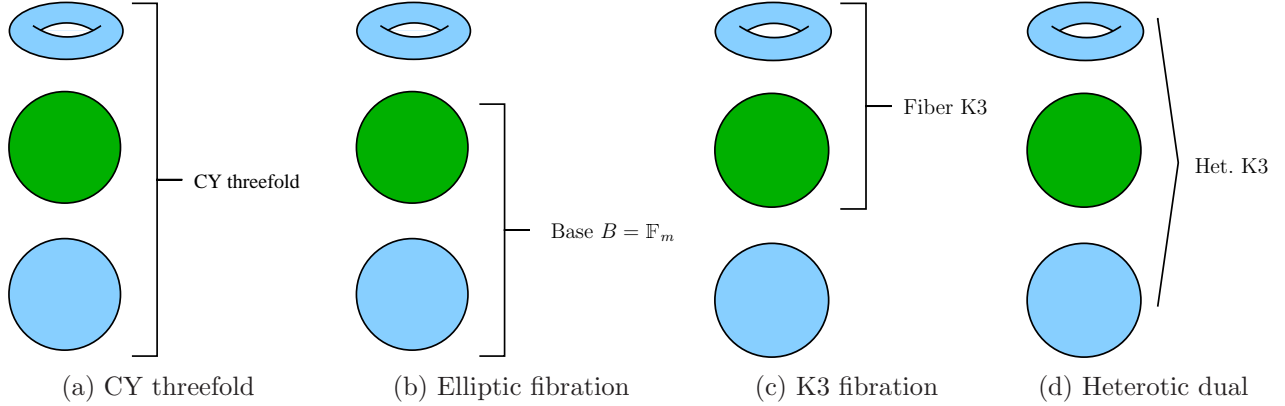


Figure 2: Picture of the CY threefold used in the F-theory construction. It is shown how the CY can be interpreted as: (b) elliptically fibered over \mathbb{F}_m , (c) K3 fibered over \mathbb{P}^1 , and (d) in terms of the heterotic K3 the theory will be dual to.

$\mathcal{N} = 1$ to the 4D $\mathcal{N} = 2$ theory, the 6D vector and tensor multiplets correspond to 4D vector multiplets while the 6D hypermultiplets stay hypermultiplets in 4D, one finds

$$N_{\text{T}} = h^{1,1}(B) - 1, \quad \text{rk}(V) = h^{1,1}(X) - h^{1,1}(B) - 1, \quad N_{\text{H}}^{\text{neutral}} = h^{2,1}(X) + 1. \quad (4)$$

Here, $\text{rk}(V)$ is the rank of the unbroken 6D gauge group and $N_{\text{H}}^{\text{neutral}}$ is the number of uncharged hypermultiplets. As explained above, models with a perturbative heterotic dual have $N_{\text{T}} = 1$. Since \mathbb{F}_m inherits the two Kähler classes of the \mathbb{P}^1 's, it has $h^{1,1}(B) = 2$, which corresponds to $N_{\text{T}} = 1$, as it should be. Furthermore, it has been argued in the smooth case that F-theory with base space \mathbb{F}_m corresponds to a heterotic $E_8 \times E_8$ theory with vector bundles where $12 + m$ instantons are embedded in the first E_8 and $12 - m$ in the second E_8 . All the models in table 1 have an unbroken hidden E_8 gauge group. For this reason, we will concentrate on \mathbb{F}_{12} where all 24 instantons are embedded in the first E_8 , leaving the second E_8 intact.

For the description of the elliptic fibered CY threefold we use the Weierstrass model. There the elliptic curve is parametrized as a sextic in the weighted projective space \mathbb{P}_{231}^2 ,

$$y^2 = x^3 + fxz^4 + gz^6, \quad (5)$$

with homogeneous coordinates x, y, z . The fibration over the base \mathbb{F}_{12} is encoded in f and g , which are appropriate sections such that the complete elliptic fibration has a trivial anticanonical bundle. The elliptic fiber degenerates at points where its discriminant

$$\Delta = 4f^3 + 27g^2 \quad (6)$$

vanishes. We summarize the scalings² of the model in table 2. For the base \mathbb{P}^1 , we denote the homogeneous coordinates by s, t and the scaling by μ . For the fiber \mathbb{P}^1 we denote the coordinates by u, v and the scaling by λ ; the scaling of the ambient space for the elliptic fiber \mathbb{P}_{231}^2 is denoted by ν .

²For \mathbb{F}_m , the λ -scaling is m for u , $2(m+2)$ for x , and $3(m+2)$ for y .

Scaling	s	t	u	v	x	y	z	f	g	Δ
λ	1	1	12	0	28	42	0	56	84	168
μ	0	0	1	1	4	6	0	8	12	24
ν	0	0	0	0	2	3	1	0	0	0

Table 2: Scalings of the homogeneous coordinates of the elliptically fibered CY threefold with base \mathbb{F}_{12} .

ord(f)	ord(g)	ord(Δ)	Name	Gauge group
0	0	n	I_n	SU(n)
≥ 2	3	$n+6$	I_n^*	SO($2n+8$)
2	≥ 3	$n+6$		
≥ 3	4	8	IV^*	E_6
3	≥ 5	9	III^*	E_7
≥ 4	5	10	II^*	E_8

Table 3: Excerpt from the Kodaira classification of the vanishing orders and the corresponding gauge groups.

From the vanishing order of (f, g, Δ) the gauge group and the matter content can be inferred according to the Kodaira classification [16], cf. table 3. In order to resolve the singular fiber at codimension 1, one glues in extra \mathbb{P}^1 's. Their intersection numbers with each other and with the original torus are given by the negative of the affine Cartan matrix of the corresponding gauge group.

2.3 Heterotic – F-theory duality in the smooth case

Before studying the singular limit we want to line out the duality in the smooth case which is much better understood [26].

Fully Higgsed case with gauge group E_8

In the generic case the entire gauge group is Higgsed. Due to the fixed chirality (and the anomaly constraint (2)) one loses one hypermultiplet per vector multiplet. Thus by assigning VEVs to the charged matter, i.e. to the $(\mathbf{56}, \mathbf{1})$ and the $(\mathbf{1}, \mathbf{2})$, we can break the visible sector gauge group completely, losing $133 + 3 = 136$ hypers and vectors. Since there is no charged matter under the second E_8 , this group stays unbroken. Thus after Higgsing, we are left with $628 - 136 = 492$ singlets, 248 vector multiplets of the second E_8 , and 1 tensor multiplet.

On the heterotic side, the 24 instantons are embedded in the whole E_8 . Thus, we expect an E_8 bundle with instanton number 24 in the correspondence. Such a bundle has 472 moduli. Together with the 20 geometric moduli of the K3, we recover the 492 singlets predicted from the F-theory side.

Let us see how to realize this situation in the Weierstrass model. In the generic case, f and g are arbitrary homogeneous polynomials in the coordinates s, t, u, v of the base. We first

expand them in u, v :

$$\frac{1}{3}f = c_{56}v^8 + c_{44}uv^7 + c_{32}u^2v^6 + c_{20}u^3v^5 + c_8u^4v^4, \quad (7a)$$

$$\frac{1}{2}g = d_{84}v^{12} + d_{72}uv^{11} + d_{60}u^2v^{10} + d_{48}u^3v^9 + d_{36}u^4v^8 + d_{24}u^5v^7 + d_{12}u^6v^6 + d_0u^7v^5. \quad (7b)$$

There can be no higher terms because u has a λ -weight of 12. The coefficients c_i, d_j are homogeneous polynomials in s, t where the degree is given by the subscripts; in particular, d_0 is just a number. With this general structure, we find for the discriminant

$$\frac{1}{4 \cdot 27}\Delta = f^3 + g^2 = v^{10}\Delta_{\text{red}}. \quad (8)$$

Hence we have an E_8 singularity at $v = 0$ and no further generic gauge group, since the reduced discriminant Δ_{red} does not factorize further and thus corresponds to an I_1 fiber degeneration, cf. table 3.

In order to check the charged hypermultiplet spectrum, we investigate how the matter curves intersect. We see that the I_1 fiber locus $\Delta_{\text{red}} = 0$ does not intersect the E_8 brane $v = 0$, since

$$\Delta_{\text{red}} \sim (d_0^2u^{14} + \mathcal{O}(v)). \quad (9)$$

Note that the monomial uv is in the Stanley–Reissner ideal and thus the two coordinates cannot vanish simultaneously. Furthermore, d_0 is just a number not equal to zero: If it were zero, $\text{ord}(\Delta) = 11$ at $v = 0$, which is too singular to allow for a crepant resolution. So there are no “brane intersections”, and we do not expect any charged matter. On the other hand, the neutral hypers can be counted by the coefficients in the the polynomials: The total number of coefficients in the c_q and d_k is 509. Subtracting three for $\text{SL}(2, \mathbb{C})$ acting on the base coordinates and 14 for $u \rightarrow \alpha u + \beta_{12}(s, t)v, v \rightarrow v/\alpha$, we end up with $509 - 3 - 14 = 492$. Hence, we reproduce the fully Higgsed heterotic model.

Furthermore, we used `palp` [27] as a cross-check to calculate the Hodge numbers of the elliptically fibered CY threefold over \mathbb{F}_{12} . We get $h^{1,1}(X) = 11$ and $h^{2,1}(X) = 491$, and $h^{1,1}(\mathbb{F}_{12}) = 2$. By comparing with (4), we find indeed that the rank of the gauge group is $\text{rk}(V) = 8$, and there are 492 neutral hypermultiplets.

Minimally Higgsed case with gauge group $E_7 \times E_8$

The largest gauge group which can be obtained in perturbative string theory on the smooth heterotic side is when all instantons are embedded in the $\text{SU}(2)$ (Alternatively, one can think of only giving VEVs to the $(\mathbf{1}, \mathbf{2})$ but not to the $(\mathbf{56}, \mathbf{1})$). This case corresponds to an $\text{SU}(2)$ bundle which leaves an unbroken gauge group of $E_7 \times E_8$. In the process of Higgsing, we break the $\text{SU}(2)$ and lose three hypers. From the spectrum in table 1, we see that we end up with $2 + 8 = 10$ $\mathbf{56}$'s and $4 + 32 \times 2 - 3 = 65$ singlets in that case.

In order to get an enhanced gauge group from the Weierstrass model, we have to restrict the polynomials. It is rather straightforward to see that we can get an E_7 singularity if we set

$$c_{56} = c_{44} = c_{32} = 0, \quad d_{84} = d_{72} = d_{60} = d_{48} = d_{36} = 0. \quad (10)$$

The determinant then factorizes as

$$\frac{1}{4 \cdot 27} \Delta = u^9 v^{10} \Delta_{\text{red}}, \quad (11)$$

and we find an E_8 at $v = 0$, an E_7 at $u = 0$, and a smooth I_1 locus at $\Delta_{\text{red}} = 0$ since it does not factorize further.

Regarding the matter spectrum, it is clear that on the one hand we have lost neutral hypermultiplets from the complex structure moduli (namely the ones in the polynomial we have set to zero), but on the other hand have gained charged matter from the resolution of the singularity enhancements where the “branes” intersect, i.e. where the singularity in the fiber gets worse. Explicitly, the remaining polynomials contain 69 parameters, but the reparameterizations that are left are just the ones on the base and a rescaling of u (since $u = 0$ should be fixed). Hence, we find $69 - 3 - 1 = 65$ neutral hypermultiplets. Regarding the charged matter, we look at the reduced determinant,

$$\begin{aligned} \Delta_{\text{red}} = & c_{20}^3 v^5 + (3c_{20}^2 c_8 + d_{24}^2) uv^4 + (3c_{20} c_8^2 + 2d_{24} d_{12}) u^2 v^3 \\ & + (c_8^3 + d_{12}^2 + 2d_{24} d_0) u^3 v^2 + 2d_{12} d_0 u^4 v + d_0^2 u^5, \end{aligned} \quad (12)$$

which intersects $u = 0$ at 20 points on the base \mathbb{P}^1 . At each of these intersection points, we expect one half-hypermultiplet of **56**, yielding 10 full **56** hypers. Since again u and v cannot vanish simultaneously, we find no intersection of the E_7 with the E_8 curve or of the E_8 with the I_1 curve.

From the cross-check with `palp` we obtain $h^{1,1} = 18$ and $h^{2,1} = 64$, which is consistent with our previous findings. We could now go back to the generic case by switching on VEVs, or polynomials, which is basically the path outlined in [26].

Completely unhiggsed case with gauge group $E_7 \times \text{SU}(2) \times E_8$

Motivated by the previous results, our ansatz is to factorize Δ_{red} further by choosing less generic polynomials such that we find an additional I_2 locus. In addition to the three extra vector multiplets, we should get three new hypermultiplets, which, together with the already-present 65 singlets of E_7 organize themselves into 32 doublets of $\text{SU}(2)$ plus four remaining singlets. However, we expect the following problems: First, from the orbifold analysis we expect fractional instantons: we need a total instanton number of 24, which should be divided evenly among the 16 \mathbb{Z}_2 fixed points which are the only loci of non-zero curvature. Hence, each fixed point carries a fractional instanton number of $24/16 = 3/2$. Furthermore, these instantons, embedded in the first E_8 , should not break the gauge group but only branch it to $E_7 \times \text{SU}(2)$. Second, the $\text{SU}(2)$ doublets, the E_7 charged matter, and the instantons are localized at the orbifold fixed points. This leads to a singularity at the intersection points in codimension two which is too severe for the usual rules of calculating the spectrum to apply. Third, due to the homogeneity of the polynomials in Δ_{red} , the extra $\text{SU}(2)$ locus will be located at the zeros of a factor of the form $(u + p_{12}v)^2 = 0$, i.e. we get a natural quantization of matter states in multiples of 12 arising from the λ -scaling of \mathbb{F}_{12} . However, the multiplicity of **(56, 2)** is 1 and the multiplicity of **(1, 2)** is 32, so neither is dividable by 12. Before we discuss how to

Gauge group	Irrep \mathbf{R}	$A_{\mathbf{R}}$	$B_{\mathbf{R}}$	$C_{\mathbf{R}}$	Normalization
SU(2)	2	1	0	$\frac{1}{2}$	1
	Adj	4	0	8	
E ₇	56	1	0	$\frac{1}{24}$	12
	Adj	3	0	$\frac{1}{6}$	
E ₈	Adj	1	0	$\frac{1}{100}$	60
SO(12)	12	1	1	0	2
	32	4	-2	$\frac{3}{2}$	
	Adj	10	4	3	

Table 4: Values of the $A_{\mathbf{R}}$, $B_{\mathbf{R}}$, and $C_{\mathbf{R}}$ used in the calculation of the anomaly polynomial.

tackle this problem in the next section, it is worthwhile to investigate other approaches to the duality to see how these problems arise there.

2.4 Comparison with other singular K3 limits

In a series of beautiful papers [17–19] a connection between the data from the anomaly polynomial and the geometry of the CY threefold was worked out. For the Green–Schwarz anomaly cancellation, the anomaly polynomial eight-form \mathfrak{I}_8 has to factorize into two four-forms as

$$\mathfrak{I}_8 = \left(\text{tr } R^2 - \sum_i \text{tr } \alpha_i F_i^2 \right) \left(\text{tr } R^2 - \sum_i \text{tr } \tilde{\alpha}_i F_i^2 \right), \quad (13)$$

where tr is the trace in the fundamental and R and F are the curvature and the field strengths, respectively. In order to get to this factorization, the traces $\text{tr}_{\mathbf{R}}$ in a representation \mathbf{R} are written in terms of traces tr in the fundamental as

$$\begin{aligned} \text{tr}_{\mathbf{R}} F^2 &= A_{\mathbf{R}} \text{tr } F^2, \\ \text{tr}_{\mathbf{R}} F^4 &= B_{\mathbf{R}} \text{tr } F^4 + C_{\mathbf{R}} (\text{tr } F^2)^2. \end{aligned} \quad (14)$$

The constants $A_{\mathbf{R}}$, $B_{\mathbf{R}}$, $C_{\mathbf{R}}$ can be calculated from group theory [18, 28], cf. table 4. Denoting the multiplicities of a state transforming in a representation (\mathbf{R}) by $x_{\mathbf{R}}$ and the multiplicities of a bi-fundamental transforming in a representation (\mathbf{R}, \mathbf{S}) by $x_{\mathbf{R}\mathbf{S}}$, the real coefficients $\alpha, \tilde{\alpha}$ in the factorized anomaly polynomial (13) have to fulfill

$$\begin{aligned} \alpha_i + \tilde{\alpha}_i &= \frac{1}{6} \left(A_{\text{adj}}^i - \sum_{\mathbf{R}} x_{\mathbf{R}}^i A_{\mathbf{R}}^i \right), \\ \alpha_i \cdot \tilde{\alpha}_i &= \frac{2}{3} \left(\sum_{\mathbf{R}} x_{\mathbf{R}}^i C_{\mathbf{R}}^i - C_{\text{adj}}^i \right), \\ \alpha_i \cdot \tilde{\alpha}_j + \alpha_j \cdot \tilde{\alpha}_i &= 4 \sum_{\mathbf{R}, \mathbf{S}} x_{\mathbf{R}\mathbf{S}}^{ij} A_{\mathbf{R}}^i A_{\mathbf{S}}^j. \end{aligned} \quad (15)$$

Since the multiplicity of the states is related to the number of intersections of matter curves, the numbers $\alpha_i, \tilde{\alpha}_i$ can be related to the divisors in \mathbb{F}_m . Following the notation in table 2, we use the integral divisor basis $D_v = \{v = 0\}$, $D_s = \{s = 0\} \sim D_t = \{t = 0\}$. Then $D_u = \{u = 0\} = D_v + mD_s$. Their intersection numbers are

$$D_v \cdot D_v = -m, \quad D_v \cdot D_s = 1, \quad D_s \cdot D_s = 0. \quad (16)$$

and the anti-canonical divisor is

$$-K = D_u + D_v + D_s + D_t = 2D_v + (2+m)D_s \quad (17)$$

The divisors ξ_i corresponding to the matter curves are linked to $(\alpha_i, \tilde{\alpha}_i)$ via

$$\xi_i = \frac{\alpha}{2} \left(D_v + \frac{m}{2} D_s \right) + \frac{\tilde{\alpha}}{2} D_s. \quad (18)$$

Applying this to the ‘‘minimally Higgsed’’ case with gauge group $E_7 \times E_8$ on \mathbb{F}_{12} , one finds

$$\begin{aligned} (\alpha_{E_7}, \tilde{\alpha}_{E_7}) = (2, 12) &\implies \xi_{E_7} = D_v + 12D_s = D_u, \\ (\alpha_{E_8}, \tilde{\alpha}_{E_8}) = (2, -12) &\implies \xi_{E_8} = D_v. \end{aligned} \quad (19)$$

Thus we find E_7 along $u = 0$ and E_8 along $v = 0$. For the matter spectrum one then finds using the intersection numbers (16) that $\xi_{E_7} \cdot \xi_{E_8} = 0$. Furthermore, using that the discriminant $\Delta = -12K$, we find for the reduced determinant $\Delta_{\text{red}} = -12\Delta - 9\xi_{E_7} - 10\xi_{E_8} = 5D_v + 60D_s$ where we used the vanishing orders given in table 3. Thus $\Delta_{\text{red}} \cdot \xi_{E_8} = 0$ and $\Delta_{\text{red}} \cdot \xi_{E_7} = 60$, which corresponds to the 20 zeros of c_{20}^3 in (12) (counted with multiplicities).

Factorizing the orbifold anomaly polynomial \mathfrak{J}_8 for the case of $E_7 \times \text{SU}(2) \times E_8$ yields $(\alpha_{\text{SU}(2)}, \tilde{\alpha}_{\text{SU}(2)}) = (\alpha_{E_7}, \tilde{\alpha}_{E_7}) = (2, 6)$ and thus $\xi_{E_7} = \xi_{\text{SU}(2)}$. Consequently, one finds that $\xi_{E_7} \cdot \xi_{E_8} = 0 = \xi_{E_8} \cdot \xi_{\text{SU}(2)}$ as it should be. Furthermore, we find $\xi_{E_7} \cdot \xi_{\text{SU}(2)} = 12$, but there is only one state transforming in the bi-fundamental **(56, 2)**. This factor of 12 is precisely the quantization in multiples of 12 noticed above. Furthermore, $\Delta_{\text{red}} = 3D_v + 36D_s$ and thus $\Delta_{\text{red}} \cdot \xi_{E_8} = 0$, which is as expected, but $\Delta_{\text{red}} \cdot \xi_{E_7} = \Delta_{\text{red}} \cdot \xi_{\text{SU}(2)} = 36$, while in the spectrum we have eight **(56, 1)** and 32 **(1, 2)**.

From the orbifold point of view, this was bound to happen. So let us see why the multiplicity comes out incorrectly even though all anomalies cancel and the anomaly polynomial factorizes in the right way. The reason is that the normalization chosen in (15) is such that all instantons are integral. But as pointed out above, we have a fractional instanton number of 3/2 at each fixed point. Without this change in normalization, one obtains

$$\begin{aligned} (\alpha_{E_7}, \tilde{\alpha}_{E_7}) = \left(\frac{1}{6}, 1 \right) &\implies \xi_{E_7} = \frac{1}{12} D_v + D_s = \frac{1}{12} D_u, \\ (\alpha_{\text{SU}(2)}, \tilde{\alpha}_{\text{SU}(2)}) = (2, 6) &\implies \xi_{\text{SU}(2)} = D_v + 12D_s = D_u, \\ (\alpha_{E_8}, \tilde{\alpha}_{E_8}) = \left(\frac{1}{30}, -\frac{1}{5} \right) &\implies \xi_{E_8} = \frac{1}{60} D_v. \end{aligned} \quad (20)$$

It can be easily checked that these ξ_i have the correct intersection numbers among each other, but they do not correspond to integral divisors in \mathbb{F}_{12} .

However, we have not yet made use of the fact that the heterotic compactification space our duality construction is based on is singular itself and that the orbifold has discrete holonomy. In [29], this is accounted for by using the torsion part of the Mordell–Weil group. The authors give the form that (f, g, Δ) have to take such that the Mordell–Weil group contains a factor of \mathbb{Z}_N or $\mathbb{Z}_N \times \mathbb{Z}_M$. Then they consider the stable degeneration limit [30, 31]. We will not go into the details of this construction and simply mention that in the stable degeneration the Hirzebruch surface \mathbb{F}_m degenerates into two Hirzebruch surfaces \mathbb{F}_m^i which intersect along a curve C_* . This curve forms together with its fibers the heterotic K3 in the large volume limit. Cast into the language of divisors (or their dual curves, which is used interchangeably by abuse of notation), this means we have divisors C_0 and C_* in \mathbb{F}_m^1 and divisors C_∞ and C_* in \mathbb{F}_m^2 , where the two C_* ’s have to be identified. The \mathbb{Z}_N singularities of the heterotic K3 surface arise from intersections of I_N curves with C_* . We are interested in the case where the Mordell–Weil group contains a \mathbb{Z}_2 factor, which has also been analyzed in [23]. We place the E_7 along $\xi_{E_7} = C_0$. Using the form of the discriminant necessary to get a \mathbb{Z}_2 factor that gives rise to the $(E_7 \times \text{SU}(2))/\mathbb{Z}_2$ gauge group [29], one finds that the I_2 curve is along $\xi_{\text{SU}(2)} = D_v + 8D_s$. This intersects $C_* \sim D_u$ eight times (no matter what m is). Hence this construction leads to the “wrong” singular K3 limit (i.e. not the one dual to the orbifold which has 16 \mathbb{Z}_2 singularities). By looking at the Euler number, we can see what is happening: the limit corresponds to $\text{K3}/\mathbb{Z}_2$ rather than T^4/\mathbb{Z}_2 . To show this let us denote the number of fixed points by k . We can calculate the Euler number of the (smooth) K3 [32] by starting from the original singular space X , subtracting the number of fixed points, dividing by the \mathbb{Z}_2 action, and gluing back in k exceptional divisors E :

$$\chi(\text{K3}^{\text{smooth}}) = \frac{\chi(X) - k}{|\mathbb{Z}_2|} + k\chi(E). \quad (21)$$

Using $\chi(\text{K3}^{\text{smooth}}) = 24$, $\chi(E) = 2$, $\chi(X = \text{K3}) = 24$, $\chi(X = T^4) = 0$, we find that $k = 8$ for $X = \text{K3}$ and $k = 16$ for $X = T^4$. This means that the global compactification obtained by using this method does not result in the heterotic dual we want to construct³.

3 F-theory duals of heterotic orbifold models

After having outlined why the previously considered constructions cannot work in our case we now describe the approach we are following instead. In order to do so it is thus instructive to take a closer look at the duality [14, 15]. As explained in figure 2, we have a double fibration structure on the F-theory side. In particular, the heterotic K3 is essentially the base \mathbb{P}^1 together with the elliptic fiber. This means that the “middle” terms in f and g , i.e. the terms $c_8 u^4 v^4$ and $d_{12} u^6 v^6$ should contain the geometric moduli of the heterotic K3. Indeed, subtracting an overall scaling, we obtain $8 + 12 = 20$ moduli. Likewise, the zeros of d_{24} and d_0 correspond to the instantons in the two E_8 ’s. Again, after subtracting an overall scaling, one obtains 24

³The same happens for the other orbifolds. In the \mathbb{Z}_3 case for example, one can show that this method produces only 6 fixed points instead of the 9 that we would expect from the orbifold, which is again consistent with a quotient $\text{K3}/\mathbb{Z}_3$ rather than T^4/\mathbb{Z}_3 .

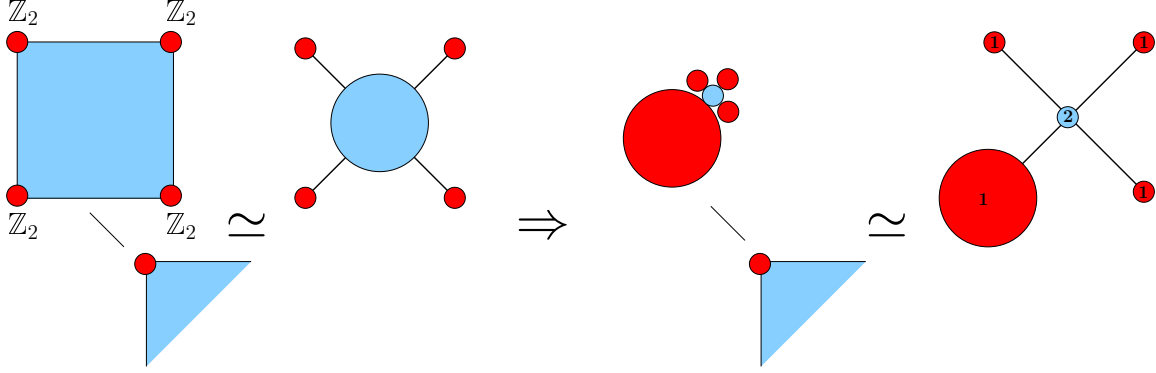


Figure 3: Blowdown limit of T^4/\mathbb{Z}_2 . Over each base singularity there is an orbifold pillow with four \mathbb{Z}_2 singularities, corresponding to the affine Dynkin diagram of $\text{SO}(8)$. In the blowdown procedure, the central torus node (blue) is blown down and one of the corner singularities (red) is blown up.

and 0, as it should be. To describe the fibration structure depicted in figure 2, we use similar methods to the ones described in [24].

3.1 Constructing the duals of the T^4/\mathbb{Z}_2 orbifold

Pictorially, the T^4/\mathbb{Z}_2 orbifold is a pillow with a torus over it everywhere except at the corners, where the fiber is a pillow itself, cf. figure 1(b). Any section will hit one of the fiber pillow corners at the base pillow corners. On the other hand, a Weierstrass fiber torus always has one singularity (at $\Delta = 0$), not four, and a non-singular section at $z = 0$. Hence we have to deform the orbifold in order to write it as a Weierstrass model. The method of [24] is to

- pick one section,
- blow up the fiber singularities it hits (such that we basically have a pillow where one of the corners is blown up to a smooth \mathbb{P}^1),
- blow down the other finite-volume component of the fiber (i.e. the original pillow).

This procedure is summarized pictorially in figure 3. In this way we end up with a fiber with a D_4 singularity (made up of three of the original pillow corners and the blown-down pillow itself), where the section sits at a smooth point. In particular, the affine node corresponds to one of the four corner singularities and the original orbifold pillow corresponds to the central (adjoint) node. Note that the central node has multiplicity (or Dynkin label) two. Hence it is intersected by a two-section rather than a section. In contrast, after applying the above procedure, we obtain a finite component with multiplicity one, which can hence be hit by a section and thus should have a Weierstrass model. This means we need to find a complex two-dimensional Weierstrass model with four D_4 singularities. We start from the heterotic Weierstrass model

$$y^2 = x^3 + \tilde{f}_8 x z^4 + \tilde{g}_{12} z^6, \quad (22)$$

where we identify $\tilde{f}_8 = c_8$ and $\tilde{g}_8 = d_{12}$ and require the vanishing orders of $(\tilde{f}, \tilde{g}, \tilde{\Delta})$ to be $(2, 3, 6)$ at four points in the base (cf. table 3). This fixes the Weierstrass equation to

$$y^2 = x^3 + \tilde{\alpha}p_4^2xz^4 + \tilde{\beta}p_4^3z^6. \quad (23)$$

Here p_4 is a polynomial of degree four in s, t , whose four zeros correspond to the position of the four fixed points in the base. The discriminant is

$$\frac{1}{4 \cdot 27} \tilde{\Delta} = (\tilde{\alpha}^3 + \tilde{\beta}^2) p_4^6, \quad (24)$$

so we clearly have four D_4 singularities at the roots of p_4 . As an additional check, note that the complex structure τ is given in terms of the j -function by

$$j(\tau) \sim \frac{\tilde{f}^3}{\tilde{\Delta}} \sim \frac{\tilde{\alpha}^3}{(\tilde{\alpha}^3 + \tilde{\beta}^2)}, \quad (25)$$

i.e. it is constant but not fixed. This fits nicely with the \mathbb{Z}_2 orbifold, in which the complex structure is also not fixed since every lattice has a reflection symmetry.

This orbifold argument fixes $c_8 = \tilde{\alpha}p_4^2$ and $d_{12} = \tilde{\beta}p_4^3$. Furthermore, we know that the 24 instantons are located at the fixed points as well, which suggests $d_{24} = \tilde{\gamma}p_4^6$. Looking at (12), we see that we have fixed all polynomials except for c_{20} . Requiring that we find an extra $SU(2)$ symmetry forces us to take $c_{20} = \tilde{\kappa}p_4^5$ and to relate the numerical coefficients $\tilde{\alpha}, \tilde{\beta}, \tilde{\gamma}, \tilde{\kappa}$ among each other. By rescaling and leaving d_0 and the coefficients in p_4 as free parameters, we then find

$$\frac{1}{3}f = \frac{4}{d_0}u^3v^4p_4^2(d_0u + 12p_4^3v), \quad (26a)$$

$$\frac{1}{2}g = \frac{1}{d_0}u^5v^5(d_0^2u^2 - 4d_0p_4^3uv - 108p_4^3v^2), \quad (26b)$$

$$\frac{1}{4 \cdot 27}\Delta = \frac{1}{d_0^3}u^9v^{10}(d_0u + 6p_4^3v)^2(d_0^3u^3 + 20d_0^2p_4^3u^2v + 68d_0p_4^6uv^2 + 3072p_4^9v^3). \quad (26c)$$

Clearly, there is an extra locus of type I_2 fibers over $d_0u + 6p_4^3v = 0$.

Spectrum

When looking at the spectrum, one has to be very careful as results may be different from what one naively expects. We present a discussion of the subtleties from different point of views. First we find that (by construction) still nothing intersects the E_8 curve at $v = 0$. However, the price to pay is that the E_7 curve, the $SU(2)$ curve, and the I_1 curve all intersect at the four points $u = 0 = p_4$. This is to be expected since all matter (except for the untwisted **(56, 2)** and the four singlets) is localized at the orbifold fixed points located at the zeros of p_4 in the base.

Now comes the tricky part: the blowup of the singularities in the base seems to introduce new tensor multiplets (whose singlets correspond to the blowup moduli), which would result in models with $N_T \neq 1$ and thus would not be dual to a perturbative heterotic model. However,

as argued by Aspinwall and Donagi in [33], the spectrum computation is much more subtle in this case. Naively one might have expected that the orbifold is the limit in which the gauge bundle becomes concentrated at the orbifold singularities, leading to point-like instantons. However, these point-like instantons are not the same as the tangent sheaf (albeit having the same support). The difference becomes apparent when looking at the spectral curve. In the former case it contains a reduced component while in the latter case it contains a fat line. This leads to different effects when resolving the singularities. In particular, in order to decide which of the multiplets (tensor, gauge, and matter multiplets) that are expected from the resolution actually do occur, one needs to investigate the corresponding extremal transitions. By studying a similar case, the authors of [33] find that the occurrence of extra tensor multiplets is indeed blocked, while the $SU(2)$ together with the four half-hyper doublets do occur.

The fact that the spectrum differs from the naive expectations can also be understood from the heterotic/M-Theory duality. Note that the instantons at the orbifold fixed points cannot be “ordinary” point-like instantons which would correspond to M5 branes. These ordinary instantons do not break or branch the gauge group; the corresponding new tensor multiplets balance the vector multiplets in the anomaly (2). This fits well with the fact that point-like instantons usually have trivial holonomy [33, 34]. In contrast, point-like instantons at orbifold singularities are expected to inherit the orbifold holonomy, which is fractional. This means that these instantons can (and do) branch the gauge group, removing some W -bosons from the spectrum. In order to still satisfy the anomaly constraint (2), no new tensor multiplets do occur. Hence these point-like instantons with non-trivial fractional holonomy cannot correspond to ordinary M5 branes. In some sense, these M5 branes with fractional holonomy are forced to sit at the fixed point with the same fractional holonomy and cannot travel through the bulk (which has trivial holonomy); hence they cannot be removed from the singularity and become ordinary M5 branes. The presence of spaces with singularities were studied in an M-theory description in [21, 35]. There, the singularities correspond to “frozen singularities” with discrete 3-form flux obstructing their resolution. It would be very interesting to construct these M-theory models directly and compare with the Jacobian of the F-theory models as discussed in [22], which is however beyond the scope of the paper.

Despite these complications, we demonstrate that the spectrum can be determined based on counting arguments as it was done in section 2.3 and is found to be as expected from the perturbative heterotic orbifold point of view. To determine the number of $\mathbf{56}$'s, we note that after deforming the extra $SU(2)$ locus away by switching on coefficients in the polynomial, we are again in the “minimally Higgsed” case described in section 2.3 with 20 $\mathbf{56}$'s, which assemble into sixteen half hypers ($\mathbf{56}, \mathbf{1}$) and one full hyper ($\mathbf{56}, \mathbf{2}$). The uncharged moduli correspond to the parameters left in the polynomials. On the heterotic side, there are four (two are related to the size and two are related to the complex structure of the $T^4 = T^2 \times T^2$ underlying the T^4/\mathbb{Z}_2 orbifold. On the F-theory side we find that there are 9 parameters: $\tilde{\alpha}, \tilde{\beta}, \tilde{\gamma}, \tilde{\kappa}, d_0$ and four parameters of p_4 . However, the zeros of p_4 are fixed as they correspond to the orbifold fixed point locations. In addition, the other parameters have to be related amongst each other for the extra $SU(2)$ locus to appear, which leaves us with four free parameters. In particular, the complex structure of the base torus depends on a combination of $\tilde{\alpha}$ and $\tilde{\beta}$, cf. (25). Finally, the doublets of $SU(2)$ are related to those deformations of the original polynomials c_{20}, c_8, d_{24} ,

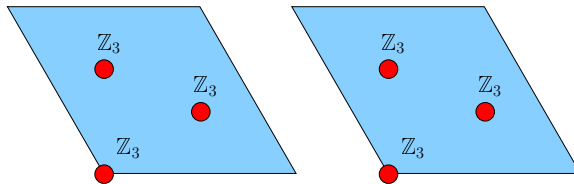


Figure 4: The orbifold T^4/\mathbb{Z}_3 has three \mathbb{Z}_3 singularities in each T^2 .

d_{12} , and d_0 that destroy the $SU(2)$ locus. As discussed in section 2.3, these have 69 parameters out of which one is an overall scaling, so there are 68. Out of these four respect the $SU(2)$ symmetry (i.e. the four singlets), so 64 parameters destroy the extra $SU(2)$ locus. These 64 correspond to the 64 half-hypers **(1, 2)**.

Stable degeneration

In terms of the stable degeneration limit, this means that the 24 I_1 fibers that generically intersect the divisor C_* are grouped into four groups with 6 I_1 's each, leading to four I_0^* singularities. Since the discriminant vanishes with order 1 along an I_1 and with order 6 along an I_0^* , we see that all 24 I_1 fiber components are used in this limit. Along the divisors C_0 we keep an E_8 fiber and along the divisor C_∞ we split the E_8 into $E_7 \times SU(2)$. When blowing up the central node in each of the I_0^* , we obtain the 16 I_2 singularities of the T^4/\mathbb{Z}_2 orbifold. It is not possible to obtain 16 I_2 directly, as this would require 32 I_1 fibers, but in a K3 there are only 24.

Of course the techniques outlined here can also be applied to other T^4/\mathbb{Z}_N orbifolds, which we will discuss now in turn.

3.2 Constructing the duals of the T^4/\mathbb{Z}_3 orbifold

We start with discussing the orbifold. It has nine \mathbb{Z}_3 (or A_2) fixed points (three per T^2 plane, cf. figure 4) and two twisted sectors,

$$\theta : (z_1, z_2) \mapsto (e^{2\pi i/3} z_1, e^{-2\pi i/3} z_2), \quad \theta^2 : (z_1, z_2) \mapsto (e^{-2\pi i/3} z_1, e^{2\pi i/3} z_2). \quad (27)$$

This means that if we distribute the instantons again evenly, we have $n_3 = 24/9 = 8/3$ instantons per fixed point or $4/3$ per resolution \mathbb{P}^1 . In order to be able to mod out the \mathbb{Z}_3 orbifold action, the complex structures of the two T^2 have to be fixed to $\tau = e^{2\pi i/3}$. For the spectrum, this means that there are two moduli (completely uncharged singlets) corresponding to the overall sizes of the tori. Since the commutant of E_8 with \mathbb{Z}_3 is $U(1)$, we find a gauge group of $E_7 \times U(1) \times E_8$. Each fixed point has one **56** and seven singlets, both charged under the $U(1)$. Furthermore, there is another **56** and another charged singlet in the untwisted sector. It can easily be checked that this satisfies the anomaly constraint (2) (as well as all other anomaly constraints, of course).

In the case where the $U(1)$ is broken, the spectrum is the same as for the \mathbb{Z}_2 model with broken $SU(2)$ (ten **56**'s and $9 \cdot 7 + 2 = 65$ singlets), so we can take the same polynomials at that stage. By the same argument as above, we cannot directly take the orbifold as a

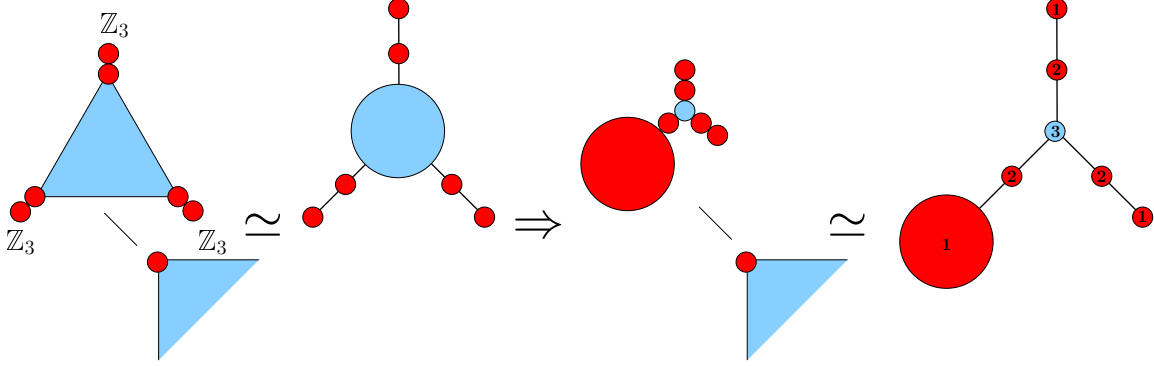


Figure 5: Blowdown limit of T^4/\mathbb{Z}_3 . Over each base singularity there is an orbifold pillow with three \mathbb{Z}_3 singularities, corresponding to the affine Dynkin diagram of E_6 . In the blowdown procedure, the central torus node (blue) is blown down and one of the corner singularities (red) is blown up.

Weierstrass model, but have to perform a similar blowup and blowdown. This time, however, the procedure takes us from nine A_2 singularities to three E_6 ones, cf. figure 5. The Dynkin label of the original finite (central) component is 3 and thus should be intersected by a three-section, while after applying the procedure, we obtain a finite component with multiplicity 1, which can be described as a Weierstrass model with a single section. The vanishing orders of \tilde{f}_8 and \tilde{g}_{12} in the heterotic Weierstrass equation (22) should be ≥ 3 and 4 at three points to obtain an E_6 . But clearly \tilde{f}_8 is not the cube of any degree-three polynomial, so we have to set $\tilde{f}_8 = 0$ (note that indeed the vanishing order for E_6 is $\text{ord}(f) \geq 3$, not necessarily equal) On the other hand, we can easily set $\tilde{g}_{12} = \alpha p_3^4$ to obtain a vanishing order of 4 at three points in the base. This has the nice effect that the the complex structure of the fiber is given by

$$j(\tau) \sim \frac{\tilde{f}_8}{\Delta} = 0, \tilde{f}_8 \quad (28)$$

i.e. it is fixed to $\tau = e^{2\pi i/3}$, just as it should be for the \mathbb{Z}_3 orbifold.

Hence we have fixed c_8 and d_{12} . Going further, we note the interpretation of d_{24} as the instanton location implies that we should have $d_{24} \sim p_3^8$, since we have 24 instantons equally divided between the three singularities, i.e. eight per singularity. On the other hand, c_{20} is again not fixed. However, by comparing to the minimally Higgsed case and to the \mathbb{Z}_2 orbifold results, we find that each zero of c_{20} contributes one **56** half-hypermultiplet, which have to combine into full hypermultiplets in this case since their $U(1)$ charge forces them into complex representations, so we make the ansatz $c_{20} \sim p_3^6 k_2$. The zeros of k_2 should then correspond to the untwisted **56**, while the p_3^6 gives rise to the twisted **56**'s. As in the \mathbb{Z}_2 case, we find that there are 18 half-hypers of **56**, one per \mathbb{P}^1 needed to resolve the \mathbb{Z}_3 singularity. Finally, the factorization should be such that there is an extra section leading to the $U(1)$ symmetry, but a detailed exploration of this is beyond the scope of this paper. The parameter counting is similar to the \mathbb{Z}_2 case (since they both have the same minimally Higgsed limit), except that there are two parameters less (corresponding to the complex structures of the two T^2 , which are fixed for this orbifold).

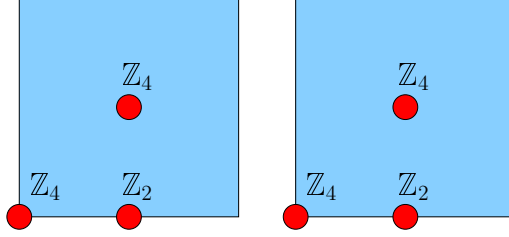


Figure 6: The orbifold T^4/\mathbb{Z}_4 has two \mathbb{Z}_4 singularities and one \mathbb{Z}_2 singularity in each T^2 .

Stable degeneration

In this case the 24 I_1 fibers are grouped into three groups with 8 I_1 's each, resulting in three IV^* singularities intersecting C_* . This uses up again all 24 I_1 fibers. Along the divisors C_0 we keep an E_8 fiber and along the divisor C_∞ we split the E_8 into $E_7 \times U(1)$. When blowing up the central node in each III^* , we obtain the 9 I_3 singularities of T^4/\mathbb{Z}_3 . Again, obtaining 9 I_3 singularities directly is impossible, since it would require 27 I_1 fibers.

3.3 Constructing the duals of the T^4/\mathbb{Z}_4 orbifold

This orbifold has three twisted sectors,

$$\theta : (z_1, z_2) \mapsto (e^{2\pi i/4} z_1, e^{-2\pi i/4} z_2), \quad \theta^2 : (z_1, z_2) \mapsto (-z_1, -z_2), \quad \theta^3 = \theta^{-1} \quad (29)$$

but the third sector is the CPT conjugate of the first, so it is enough to discuss the first and second twisted sector. In the first sector, we have two \mathbb{Z}_4 fixed points (which are at the same time \mathbb{Z}_2 fixed points of the second twisted sector) and one \mathbb{Z}_2 fixed point (cf. figure 6). For the underlying T^2 's to be compatible with the \mathbb{Z}_4 action, the complex structure of the tori have to be fixed to $\tau = i$. Picking one T^2 as the base and the other one as the fiber as before, this means that there are

- two points on the base over which there is a “ \mathbb{Z}_4 fiber”, with two \mathbb{Z}_4 and one \mathbb{Z}_2 singularities, which in blowup lead to an extended E_7 diagram (cf. figure 7),
- and one point in the base over which we have the known “ \mathbb{Z}_2 fiber”, leading to the extended D_4 diagram (cf. figure 3).

Again, this takes us from a finite component with multiplicity 4 to a finite component with multiplicity 1 in the \mathbb{Z}_4 fibers; for the \mathbb{Z}_2 fiber, the story is as in the T^4/\mathbb{Z}_2 case. The required vanishing orders of $(\tilde{f}_8, \tilde{g}_{12}, \tilde{\Delta})$ for the Weierstrass model on the heterotic side are $(3, \geq 5, 9)$ for E_7 and $(2, \geq 3, 6)$ for D_4 . Since there are two \mathbb{Z}_4 and one \mathbb{Z}_2 fiber, the combined vanishing orders are $(8, 13, 24)$. However, \tilde{g}_{12} is a section in $12D_u$; hence it cannot vanish to order 13 and we have to set $\tilde{g}_{12} = 0$ identically. This means that the complex structure of the fibration is again fixed since $\tilde{\Delta} = 4\tilde{f}^3$, and thus

$$j(\tau) \sim \frac{\tilde{f}^3}{f^3} = 1 \quad (30)$$

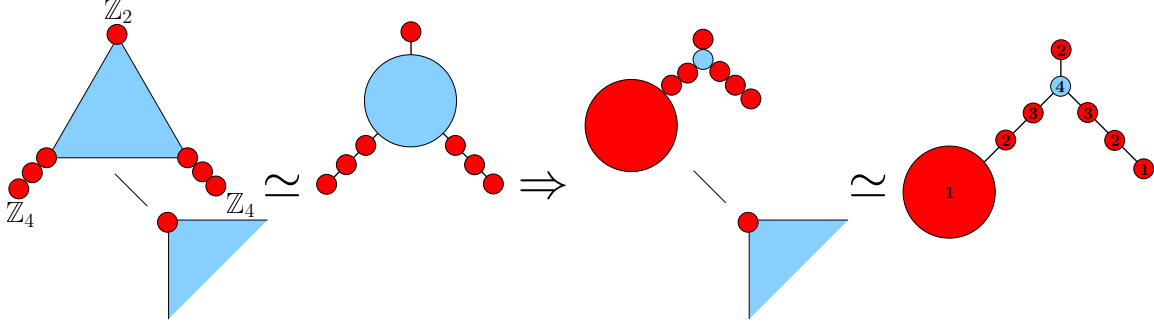


Figure 7: Blowdown limit of T^4/\mathbb{Z}_4 . Over a base singularity there is an orbifold pillow with two \mathbb{Z}_4 (one of which is depicted here) and one \mathbb{Z}_2 (depicted in figure 3) singularities, corresponding to the affine Dynkin diagram of E_7 . In the blowdown procedure, the central torus node (blue) is blown down and one of the corner singularities (red) is blown up.

From the properties of the j function, this implies that indeed $\tau = i$.

In summary, we have

$$c_8 = \tilde{f}_8 = \alpha p_1^3 q_1^3 r_1^2, \quad d_{12} = \tilde{g}_{12} = 0. \quad (31)$$

Here, p_1, q_1 , and r_1 are all polynomials of degree one, giving the locations of the two E_7 and the D_4 fiber, respectively. Again, the instantons are located at the singular fibers, so

$$d_{24} = \beta p_1^i q_1^i r_1^j \quad (32)$$

with $2i + j = 24$. Since $r_1 = 0$ is a \mathbb{Z}_2 fiber, we may assume just as for the \mathbb{Z}_2 orbifold above that $j = 6$ and thus $i = 9$, i.e. nine instantons per \mathbb{Z}_4 fiber. Using that the \mathbb{Z}_2 fixed points carry $n_2 = \frac{3}{2}$ instantons, we find that each \mathbb{Z}_4 fixed point carries $n_4 = \frac{15}{4}$ instantons (and thus $\frac{5}{4}$ instantons per resolution \mathbb{P}^1), such that $2n_4 + n_2 = 9$. We thus find that \mathbb{Z}_4 fixed points carry fractional (quarter) instantons, as seems reasonable.

Finally, using again that the half-hypers **56** are localized at the zeros of c_{20} , we expand it in powers of p_1, q_1, r_1 . Assuming that each \mathbb{P}^1 needed in the resolution process comes with one twisted **56** half-hyper as in the previous cases, we find that

$$c_{20} = \gamma p_1^7 q_1^7 r_1^4 k_2, \quad (33)$$

where again k_2 is a degree-two polynomial accounting for the untwisted **56**, which cannot be composed out of two half-hypers because of its $U(1)$ charge. Note, however, that p_1 and q_1 are raised to odd powers. This means that some of these have to correspond to actual half-hypermultiplets, which consequently cannot be charged under $U(1)$. The contributions to the massless spectrum are as follows:

- A \mathbb{Z}_4 fixed point contains three \mathbb{P}^1 's, one of which can be thought of as a \mathbb{P}^1 corresponding to the \mathbb{Z}_2 fixed point (i.e. belonging to the second twisted sector). Thus, each \mathbb{Z}_4 point contains a full **56** for the first twisted sector and a half **56** for the θ^2 sector.
- The pure \mathbb{Z}_2 fixed points simply contain half **56**'s, corresponding to the θ^2 sector.

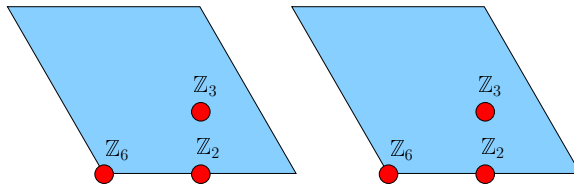


Figure 8: The orbifold T^4/\mathbb{Z}_6 has one \mathbb{Z}_6 , one \mathbb{Z}_3 , and one \mathbb{Z}_2 singularity in each T^2 .

Adding these up, we find four full **56**'s in the θ sector and $4+2(1+1+1) = 10$ half-hypers in the θ^2 sector, which matches precisely the spectrum of the orbifold, cf. table 1 and the discussion of the distribution of the **56**'s in section 2.1. The counting of parameters is as in the \mathbb{Z}_3 case. Again, we find that there are only two uncharged singlets (geometric moduli), corresponding to the sizes of the tori; the other two singlets corresponding to the complex structure are lost since it had to be fixed to be compatible with the \mathbb{Z}_4 action.

Stable degeneration

Here we group the 24 I_1 fibers into two groups with 9 I_1 's each and one group with 6 I_1 's, resulting in two III^* and one I_0^* singularities intersecting C_* . This uses up again all 24 I_1 fibers. As before, we keep the E_8 fiber along C_0 and split the other E_8 along C_∞ into $E_7 \times U(1)$. When blowing up the central nodes, we obtain 4 I_4 and 6 I_2 singularities. Again, obtaining these singularities directly would require 28 I_1 fibers intersecting C_* .

3.4 Constructing the duals of the T^4/\mathbb{Z}_6 orbifold

Lastly, we want to discuss the \mathbb{Z}_6 orbifold. Here, the orbifold action introduces one fixed point of each order \mathbb{Z}_6 , \mathbb{Z}_3 and \mathbb{Z}_2 (cf. figure 8) in each torus,

$$\begin{aligned} \theta &: (z_1, z_2) \mapsto (e^{2\pi i/6} z_1, e^{-2\pi i/6} z_2), & \theta^2 &: (z_1, z_2) \mapsto (e^{2\pi i/3} z_1, e^{-2\pi i/3} z_2), \\ \theta^3 &: (z_1, z_2) \mapsto (z_1, -z_2), & \theta^4 &= \theta^{-2}, & \theta^5 &= \theta^{-1}. \end{aligned} \quad (34)$$

The θ^4 sector is the CPT conjugate of the θ^2 sector, and the θ^5 sector is the CPT conjugate of the θ sector, so it is enough to discuss only the first three twisted sectors.

Fiberwise, this gives

- one “ \mathbb{Z}_6 fiber” with the three fixed points, leading to an E_8 fiber after performing the blowup/blowdown procedure with vanishing orders (4, 5, 10) (cf. figure 9),
- one “ \mathbb{Z}_3 fiber” which turns into an E_6 with vanishing orders (3, 4, 8) as discussed in section 3.2, and
- one “ \mathbb{Z}_2 fiber”, which becomes the D_4 fiber with vanishing orders (2, 3, 6) as discussed in section 3.1.

For the \mathbb{Z}_6 fiber, this takes us from a finite component with multiplicity 6 to a finite component with multiplicity 1; the outcome of the procedure for the other fiber types are as discussed in

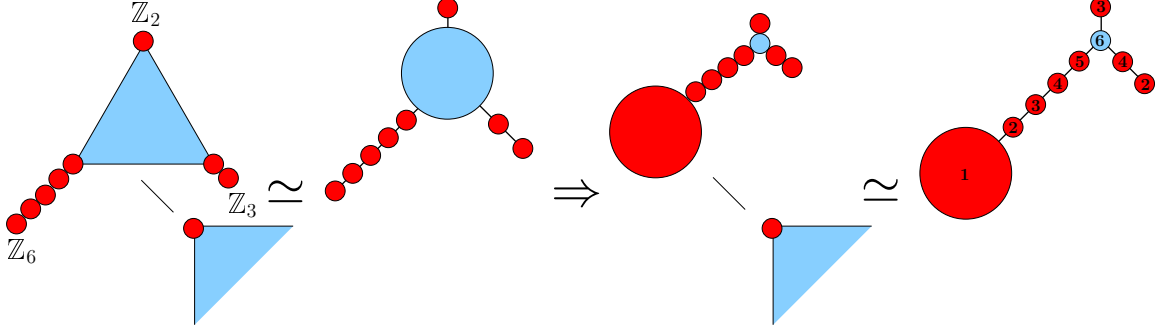


Figure 9: Blowdown limit of T^4/\mathbb{Z}_6 . Over a base singularity there is an orbifold pillow with one \mathbb{Z}_6 (depicted here), one \mathbb{Z}_3 (depicted in figure 5), and one \mathbb{Z}_2 (depicted in figure 3) singularity, corresponding to the affine Dynkin diagram of E_8 . In the blowdown procedure, the central torus node (blue) is blown down and one of the corner singularities (red) is blown up.

the previous cases. We observe in general that in the description of the \mathbb{Z}_N singularities in a T^4/\mathbb{Z}_N orbifold, we obtain Dynkin diagrams in which the original orbifold corresponds to the “central” node (i.e. the node with the most neighboring nodes) which always has a Dynkin label of N .

The overall vanishing orders of $(\tilde{f}_8, \tilde{g}_{12}, \tilde{\Delta})$ would have to be $(9, 12, 24)$, which is impossible since \tilde{f}_8 is a section in $8D_u$. Hence $\tilde{f}_8 = 0$ identically, which again fixes $\tau = e^{2\pi i/3}$ as required by the \mathbb{Z}_6 orbifold action (albeit for a different reason than in the \mathbb{Z}_3 case). We choose

$$d_{12} = \tilde{g}_{12} = \alpha p_1^5 q_1^4 r_1^3, \quad (35)$$

such that the \mathbb{Z}_6 , \mathbb{Z}_3 , and \mathbb{Z}_2 fixed points are located at the zeros of p_1 , q_1 , and r_1 , respectively.

The other polynomials are now relatively straightforward. By similar reasoning as above, we find

$$d_{24} = \beta p_1^{10} q_1^8 r_1^6. \quad (36)$$

Hence, the \mathbb{Z}_6 fiber carries ten instantons. If we want to turn this into a fixed point instanton number n_6 , we use that according to our previous results $n_3 = \frac{8}{3}$ and $n_2 = \frac{3}{2}$ and thus $n_6 = 10 - \frac{8}{3} - \frac{3}{2} = \frac{35}{6}$, which amounts to $\frac{7}{6}$ per \mathbb{P}^1 glued in to resolve the A_5 singularity. This leads to an obvious pattern: A \mathbb{Z}_k fixed point carries instanton number

$$n_k = \frac{k^2 - 1}{k}. \quad (37)$$

The \mathbb{P}^1 's glued into the corresponding A_{k-1} singularity thus carry an instanton number of $\frac{k^2-1}{k(k-1)} = \frac{k+1}{k}$, if distributed evenly.

Finally, we discuss the charged matter. To fix c_{20} we use again that each \mathbb{P}^1 used to resolve a \mathbb{Z}_N singularity contributes one half-hyper **56**. Hence we find

$$c_{20} = \gamma p_1^8 q_1^6 r_1^4 k_2. \quad (38)$$

The distribution of the **56**'s among the sectors and fixed points is then as follows:

- The untwisted sector has one **56**, corresponding to k_2 ,
- the θ sector has as its only fixed point the \mathbb{Z}_6 fixed point at $p_1 = 0$, so we expect eight, minus the \mathbb{Z}_2 and \mathbb{Z}_3 fixed points in the \mathbb{Z}_6 fiber which do not appear in the θ sector, minus the \mathbb{Z}_2 and \mathbb{Z}_3 components inside the \mathbb{Z}_6 , such that we end up with $8 - 1 - 2 - 1 - 2 = 2$ half-hypers, which can come as one charged multiplet,
- the θ^2 sector contains the \mathbb{Z}_3 fixed points at $q_1 = 0$, plus the ones in the \mathbb{Z}_6 fiber, so $6 + 2 + 2 = 10$ half-hypers, again possibly charged,
- and finally the θ^3 sector picks up the remaining $4 + 1 + 1 = 6$ half-hypers, which actually are true half-hypers, i.e. uncharged.

This agrees perfectly with the orbifold spectrum given in table 1.

Stable degeneration

Here we group the 24 I_1 fibers into a group with 10 I_1 's, a group with 8 I_1 's, and a group with 6 I_1 's, resulting in one II^* , one III^* , and one I_0^* singularity intersecting C_* , which uses up all 24 I_1 fibers as in the previous cases. Again, we keep the E_8 fiber along C_0 and split the E_8 along C_∞ into $E_7 \times U(1)$. When blowing up the central nodes, we obtain 1 I_6 , 4 I_3 , and 5 I_2 singularities, whose direct construction would require 28 I_1 fibers.

3.5 Constructing the duals of T^4/\mathbb{Z}_N orbifolds with Wilson lines

As a last step we want to discuss orbifold models with Wilson lines. If one turns on Wilson lines at the orbifold, they further branch the gauge group and project out some of the matter states. As an example, we will discuss the T^4/\mathbb{Z}_2 orbifold where one Wilson line $W = (0^2, 1, 0^5)(0^8)$ along one of the torus directions (say $e_1 = \text{Re}(z_1)$) has been switched on in addition to the standard embedding shift vector V . As a result, the $2 \times 4 = 8$ \mathbb{Z}_2 fixed points located at $e_1 = 0$ do not feel the Wilson line and behave as if it was not switched on, while the other 8 \mathbb{Z}_2 fixed points at $e_1 = \frac{1}{2}$ feel both the shift and the Wilson line. As a result, we get a gauge group of $SO(12) \times SU(2) \times SU(2)' \times E_8$ with the matter content given in table 1. Note that the $SU(2)$ corresponds to the factor branched off the E_7 , while the $SU(2)'$ corresponds to the “original“ $SU(2)$ of the above \mathbb{Z}_2 example. At the 8 fixed point where the Wilson line does not act (corresponding to the upper line in the third column of the T^4/\mathbb{Z}_2 case in table 1), the spectrum is simply branched, which means that $(\mathbf{56}, \mathbf{1}) \rightarrow 2(\mathbf{12}, \mathbf{1}) + (\mathbf{32}, \mathbf{1})$. At the other 8 fixed points, it has been calculated using the standard CFT techniques.

Hence the discussion is not as symmetric as in the first case. Nevertheless, the idea is similar. One starts with an $SO(12)$ (i.e. I_2^*) singularity at $u = 0$ with vanishing orders $(2, 3, 8)$ and an E_8 singularity at $v = 0$ and factorizes the discriminant further by restricting the polynomials until two further I_2 loci appear which correspond to the two $SU(2)$'s. The resulting expressions

f, g, Δ then are of the form

$$f \propto u^2 v^4 p_4^2 (a_1 u^2 + a_2 p_4^3 u v + a_3 p_4^6 v^2) , \quad (39a)$$

$$g \propto u^3 v^5 (a_4 d_0 u^4 + \dots + a_8 p_4^{12} v^4) , \quad (39b)$$

$$\Delta \propto u^8 v^{10} (u + a_9 p_4^3 v)^2 (u - a_9 p_4^3 v)^2 (a_{10} d_0 u^2 + \dots + a_{12} p_4^6 v^2) , \quad (39c)$$

where the a_i are (fixed) numerical constants that are determined such that the discriminant factorizes into two quadratic pieces plus a rest and that the terms containing u^6 and u^7 cancel from the discriminant, enhancing D_4 to D_6 . We thus obtain an E_8 singularity at $v = 0$, a D_6 singularity at $u = 0$ and two I_2 singularities at $u \pm a_9 p_4^3 v = 0$.

Applying the methods described in section 2.4 does again not give rise to the “correct” orbifold limit. Using table 4, we find

$$\begin{aligned} (\alpha_{\text{SO}(12)}, \tilde{\alpha}_{\text{SO}(12)}) = (2, 12) &\quad \Rightarrow \quad \xi_{\text{SO}(12)} = D_v + 12D_s = D_u , \\ (\alpha_{\text{SU}(2)}, \tilde{\alpha}_{\text{SU}(2)}) = (2, 12) &\quad \Rightarrow \quad \xi_{\text{SU}(2)} = D_v + 12D_s = D_u , \\ (\alpha_{\text{SU}(2)'}, \tilde{\alpha}_{\text{SU}(2)'}) = (2, 12) &\quad \Rightarrow \quad \xi_{\text{SU}(2)'} = D_v + 12D_s = D_u , \\ (\alpha_{E_8}, \tilde{\alpha}_{E_8}) = (2, -12) &\quad \Rightarrow \quad \xi_{E_8} = D_v . \end{aligned} \quad (40)$$

As expected, the $\text{SO}(12)$ and the two $\text{SU}(2)$'s are in the same divisor class D_u , and the E_8 is in the divisor class D_v . We thus find that

$$\begin{aligned} \xi_{\text{SO}(12)} \cdot \xi_{E_8} = \xi_{\text{SU}(2)} \cdot \xi_{E_8} = \xi_{\text{SU}(2)'} \cdot \xi_{E_8} &= 0 , \\ \xi_{\text{SO}(12)} \cdot \xi_{\text{SU}(2)} = \xi_{\text{SO}(12)} \cdot \xi_{\text{SU}(2)'} = \xi_{\text{SU}(2)} \cdot \xi_{\text{SU}(2)'} &= 12 . \end{aligned} \quad (41)$$

Neglecting again the normalization such that fractional instantons can arise we find that $\xi_{\text{SO}(12)} = \frac{1}{2}D_u$, $\xi_{\text{SU}(2)} = \xi_{\text{SU}(2)'} = D_u$, $\xi_{E_8} = \frac{1}{60}D_v$, which gives the correct spectrum.

3.6 General instanton embedding

So far we have restricted our discussion to the case where all instantons are embedded in one E_8 . In an orbifold with general gauge shift and Wilson lines, both E_8 's will be broken. Such models can also be connected to the ones we discussed here via a sequence of blowups and blowdowns in the base [14, 15, 20]. By blowing up an extra point in the base, we can get from \mathbb{F}_N to $\mathbb{F}_{N\pm 1}$. The corresponding picture in the Hořava–Witten picture of M-theory [36–38] is the following: the blowup in the base introduces an extra tensor multiplet; the scalar of this tensor multiplet encodes the position of on M5 brane in the M-theory bulk (i.e. on the interval between the two E_8 branes). Thus by blowing up and blowing down, we can “peel off” an M5 brane from one E_8 (blowup), let it travel through the bulk, and absorb it at the other E_8 brane (blowdown), changing the instanton embedding in this way. For the analysis, this means that the expansions in (7) have to be done such that they are compatible with the new scalings. The geometry of the singularity structure does not change, and the terms in the expansions can still be identified with bundle and geometry data [15].

4 Conclusions and outlook

In this paper we investigated heterotic models compactified on singular K3 spaces corresponding to abelian toroidal orbifolds T^4/\mathbb{Z}_N and argued that all these models can be connected via F-theory.

For the sake of simplicity we concentrated on the standard embedding of these orbifolds, in which one E_8 is broken rank-preservingly to either $E_7 \times \text{SU}(2)$ or $E_7 \times \text{U}(1)$ and the other E_8 is left unbroken. First we discussed previous approaches for constructing F-theory duals of smooth heterotic K3 models and argued why these approaches cannot be used. For the construction of the duals, we first had to describe the geometry of the T^4/\mathbb{Z}_N models on the heterotic side. Having singular fibers by itself over singularities in the base, the description led to fibers with singularities of the type I_0^* , IV^* , III^* and II^* . By calculating the $j(\tau)$ function of these fibers, we found that the complex structure of the orbifold torus is free in the T^4/\mathbb{Z}_2 case, fixed to $\tau = e^{2\pi i/3}$ in the T^4/\mathbb{Z}_3 and T^4/\mathbb{Z}_6 case, and fixed to $\tau = i$ in the T^4/\mathbb{Z}_4 case, as needed for compatibility with the orbifold action. We found that in these constructions the node corresponding to the “orbifold pillow” in a fiber above a \mathbb{Z}_N singularity in the base has multiplicity N . Furthermore, the distribution of the fractional instantons over the \mathbb{Z}_N fixed points in the base is $(N^2 - 1)/N$.

By blowing down the “orbifold pillow” and blowing up one of the Dynkin nodes with multiplicity one, we could go to a Weierstrass description of the model. Using the information about the instanton embeddings and the singularities of the geometry on the heterotic side, we could tune the complex structure parameters on the F-theory side such that the defining quantities (f, g, Δ) of the F-theory Weierstrass model have the vanishing orders needed to reproduce the gauge groups on the heterotic side.

However, the resulting models were too singular to apply the usual spectrum calculation rules of F-theory. The reason is that (most) matter and instantons are living at the singularities on the heterotic side and thus all components of the discriminant on the F-theory side vanish at the fixed point loci of the heterotic dual. Nevertheless, by counting parameters and deforming the singularities away to connect to the (partially Higgsed) smooth model, we argued that the F-theory spectrum coincides with the spectrum on the heterotic side. Using the strong constraints imposed by 6D anomaly cancellation, we could further cross-check the spectrum. The results obtained from the counting agree with the ones obtained by Aspinwall and Donagi in [33] for F-theories with orbifold singularities in the fiber.

In the end, we investigated more general gauge sectors with Wilson lines and configurations in which both E_8 's were broken on the heterotic side and argued that these can be obtained by further specialization of the complex structure moduli in the CY threefold combined with blowups and blowdowns in the base \mathbb{F}_N . In particular, the geometry on the heterotic side and the gauge group and matter content in each E_8 are described by the complex structure on the F-theory side, while the instanton embedding on the heterotic side corresponds to blowups and blowdowns in the base on the F-theory side. This means that heterotic orbifold Wilson lines map to complex structure parameters (and not to Wilson lines) on the F-theory side.

Outlook

It should be noted that the methods we applied here for the description of the geometry of the singular K3 compactifications could in principle also be applied to CY threefolds on the heterotic side (of course there the anomaly cancellation conditions are weaker, which makes cross-checking the F-theory matter spectrum harder). It would be very interesting to see which of the T^6/\mathbb{Z}_N and $T^6/(\mathbb{Z}_N \times \mathbb{Z}_M)$ orbifolds are connected via F-theory on CY fourfolds.

In addition, one could work out the description of the heterotic orbifolds and their F-theory duals directly using multisections as recently explored in [22] rather than constructing the Weierstrass model using the blowup and blowdown procedure, and match the results.

Furthermore, it would be interesting to study the M-theory description of these models and compare it with the the case of frozen singularities and discrete 3-form flux [21, 35].

Acknowledgments

We thank Andreas Braun, Volker Braun, and Iñaki García Etxebarria for helpful discussions and Denis Klevers for comments on the manuscript. The work of FR was supported by the German Science Foundation (DFG) within the Collaborative Research Center (SFB) 676 “Particles, Strings and the Early Universe”.

References

- [1] L. J. DIXON, J. A. HARVEY, C. VAFA AND E. WITTEN, “Strings on Orbifolds,” *Nucl.Phys.* **B261** (1985) 678–686.
- [2] L. J. DIXON, J. A. HARVEY, C. VAFA AND E. WITTEN, “Strings on Orbifolds. 2.,” *Nucl.Phys.* **B274** (1986) 285–314.
- [3] L. E. IBANEZ, H. P. NILLES AND F. QUEVEDO, “Orbifolds and Wilson Lines,” *Phys.Lett.* **B187** (1987) 25–32.
- [4] W. BUCHMULLER, K. HAMAGUCHI, O. LEBEDEV AND M. RATZ, “Supersymmetric standard model from the heterotic string,” *Phys.Rev.Lett.* **96** (2006) 121602 [[hep-ph/0511035](#)].
- [5] W. BUCHMULLER, K. HAMAGUCHI, O. LEBEDEV AND M. RATZ, “Supersymmetric Standard Model from the Heterotic String (II),” *Nucl.Phys.* **B785** (2007) 149–209 [[hep-th/0606187](#)].
- [6] O. LEBEDEV, H. P. NILLES, S. RABY, S. RAMOS-SANCHEZ, M. RATZ AND OTHERS, “A Mini-landscape of exact MSSM spectra in heterotic orbifolds,” *Phys.Lett.* **B645** (2007) 88–94 [[hep-th/0611095](#)].
- [7] O. LEBEDEV, H. P. NILLES, S. RAMOS-SANCHEZ, M. RATZ AND P. K. VAUDREVANGE, “Heterotic mini-landscape. (II). Completing the search for MSSM vacua in a $Z(6)$ orbifold,” *Phys.Lett.* **B668** (2008) 331–335 [[0807.4384](#)].
- [8] M. BLASZCZYK, S. GROOT NIBBELINK, M. RATZ, F. RUEHLE, M. TRAPLETTI AND OTHERS, “A $Z_2 \times Z_2$ standard model,” *Phys.Lett.* **B683** (2010) 340–348 [[0911.4905](#)].
- [9] H. M. LEE, S. RABY, M. RATZ, G. G. ROSS, R. SCHIEREN AND OTHERS, “A unique Z_4^R symmetry for the MSSM,” *Phys.Lett.* **B694** (2011) 491–495 [[1009.0905](#)].
- [10] D. LUST, S. REFFERT, E. SCHEIDEGGER AND S. STIEBERGER, “Resolved Toroidal Orbifolds and their Orientifolds,” *Adv.Theor.Math.Phys.* **12** (2008) 67–183 [[hep-th/0609014](#)].

- [11] S. GROOT NIBBELINK, D. KLEVERS, F. PLOGER, M. TRAPLETTI AND P. K. VAUDREVANGE, “Compact heterotic orbifolds in blow-up,” *JHEP* **0804** (2008) 060 [[0802.2809](#)].
- [12] M. BLASZCZYK, S. GROOT NIBBELINK AND F. RUEHLE, “Gauged Linear Sigma Models for toroidal orbifold resolutions,” *JHEP* **1205** (2012) 053 [[1111.5852](#)].
- [13] C. VAFA, “Evidence for F theory,” *Nucl.Phys.* **B469** (1996) 403–418 [[hep-th/9602022](#)].
- [14] D. R. MORRISON AND C. VAFA, “Compactifications of F theory on Calabi-Yau threefolds. 1,” *Nucl.Phys.* **B473** (1996) 74–92 [[hep-th/9602114](#)].
- [15] D. R. MORRISON AND C. VAFA, “Compactifications of F theory on Calabi-Yau threefolds. 2.,” *Nucl.Phys.* **B476** (1996) 437–469 [[hep-th/9603161](#)].
- [16] K. KODAIRA, “On compact analytic surfaces,” *Annals of Mathematics* **77** (1963) 563.
- [17] V. KUMAR, D. R. MORRISON AND W. TAYLOR, “Mapping 6D $N = 1$ supergravities to F-theory,” *JHEP* **1002** (2010) 099 [[0911.3393](#)].
- [18] W. TAYLOR, “Anomaly constraints and string/F-theory geometry in 6D quantum gravity,” [[1009.1246](#)].
- [19] V. KUMAR, D. R. MORRISON AND W. TAYLOR, “Global aspects of the space of 6D $N = 1$ supergravities,” *JHEP* **1011** (2010) 118 [[1008.1062](#)].
- [20] N. SEIBERG AND E. WITTEN, “Comments on string dynamics in six-dimensions,” *Nucl.Phys.* **B471** (1996) 121–134 [[hep-th/9603003](#)].
- [21] J. DE BOER, R. DIJKGRAAF, K. HORI, A. KEURENTJES, J. MORGAN AND OTHERS, “Triples, fluxes, and strings,” *Adv.Theor.Math.Phys.* **4** (2002) 995–1186 [[hep-th/0103170](#)].
- [22] V. BRAUN AND D. R. MORRISON, “F-theory on Genus-One Fibrations,” [[1401.7844](#)].
- [23] M. MARQUART AND D. WALDRAM, “F theory duals of M theory on $S^{*1} / Z(2) \times T^{*4} / Z(N)$,” [[hep-th/0204228](#)].
- [24] A. P. BRAUN, R. EBERT, A. HEBECKER AND R. VALANDRO, “Weierstrass meets Enriques,” *JHEP* **1002** (2010) 077 [[0907.2691](#)].
- [25] G. HONECKER AND M. TRAPLETTI, “Merging Heterotic Orbifolds and K3 Compactifications with Line Bundles,” *JHEP* **0701** (2007) 051 [[hep-th/0612030](#)].
- [26] M. BERSHADSKY, K. A. INTRILIGATOR, S. KACHRU, D. R. MORRISON, V. SADOV AND OTHERS, “Geometric singularities and enhanced gauge symmetries,” *Nucl.Phys.* **B481** (1996) 215–252 [[hep-th/9605200](#)].
- [27] M. KREUZER AND H. SKARKE, “PALP: A Package for analyzing lattice polytopes with applications to toric geometry,” *Comput.Phys.Commun.* **157** (2004) 87–106 [[math/0204356](#)].
- [28] J. ERLER, “Anomaly cancellation in six-dimensions,” *J.Math.Phys.* **35** (1994) 1819–1833 [[hep-th/9304104](#)].
- [29] P. S. ASPINWALL AND D. R. MORRISON, “Nonsimply connected gauge groups and rational points on elliptic curves,” *JHEP* **9807** (1998) 012 [[hep-th/9805206](#)].
- [30] R. FRIEDMAN, J. MORGAN AND E. WITTEN, “Vector bundles and F theory,” *Commun.Math.Phys.* **187** (1997) 679–743 [[hep-th/9701162](#)].
- [31] P. S. ASPINWALL AND D. R. MORRISON, “Point - like instantons on K3 orbifolds,” *Nucl.Phys.* **B503** (1997) 533–564 [[hep-th/9705104](#)].
- [32] M. B. GREEN, J. H. SCHWARZ AND E. WITTEN, *Superstring theory vol. 2: Loop amplitudes, anomalies and phenomenology*. Cambridge, Uk: Univ. Pr. 596 P. (Cambridge Monographs On Mathematical Physics) 1987.

- [33] P. S. ASPINWALL AND R. Y. DONAGI, “The Heterotic string, the tangent bundle, and derived categories,” *Adv.Theor.Math.Phys.* **2** (1998) 1041–1074 [[hep-th/9806094](#)].
- [34] P. S. ASPINWALL, “K3 surfaces and string duality,” [[hep-th/9611137](#)].
- [35] E. WITTEN, “Toroidal compactification without vector structure,” *JHEP* **9802** (1998) 006 [[hep-th/9712028](#)].
- [36] P. HORAVA AND E. WITTEN, “Heterotic and type I string dynamics from eleven-dimensions,” *Nucl.Phys.* **B460** (1996) 506–524 [[hep-th/9510209](#)].
- [37] P. HORAVA AND E. WITTEN, “Eleven-dimensional supergravity on a manifold with boundary,” *Nucl.Phys.* **B475** (1996) 94–114 [[hep-th/9603142](#)].
- [38] A. KLEMM, P. MAYR AND C. VAFA, “BPS states of exceptional noncritical strings,” [[hep-th/9607139](#)].